FORCE–DISPLACEMENT RELATIONSHIP IN THE EXTRACTION
OF A PORCINE TOOTH FROM ITS SOCKET:
EXPERIMENTS AND NUMERICAL SIMULATIONS

Francesco Genna and Corrado Paganelli

FORCE–DISPLACEMENT RELATIONSHIP IN THE EXTRACTION OF A PORCINE TOOTH FROM ITS SOCKET: EXPERIMENTS AND NUMERICAL SIMULATIONS

FRANCESCO GENNA AND CORRADO PAGANELLI

Results of new investigations about the global tensile stiffness and strength of the periodontal ligament are presented. Experimental results are reported first, referring to the extraction of swine teeth from their sockets: force–displacement curves are shown, obtained from samples including a portion of the jaw and a canine swine tooth. Numerical simulations of the same tooth extraction tests are then presented, which exploit specific modelling techniques previously developed. In particular, use is made of an interface finite element capable to describe the fibrous structure of the periodontal ligament, and of a stress–stretch constitutive model, for a single collagen fibre, based on the multiscale nature of its subfibrillar microstructure. The comparison between the new experimental results and the numerical ones helps in understanding the soundness of the adopted mechanical models in the simulations. This study is expected to be mainly useful in providing results usable for the indirect validation of mechanical models of both the periodontal ligament and its basic constituent, the single collagen fibre.

1. Introduction

The periodontal ligament (PDL) is, among the components of the masticatory system, the one that most profoundly influences and determines the mechanical behaviour of the system itself. This is because the PDL is the most compliant component in this system, and because it exhibits a strongly anisotropic and nonlinear response to applied mechanical actions.

Dental mechanics is still singularly lacking systematic and extensive contributions to the study of the mechanical behaviour of the PDL, especially in humans. Some experimental results are available, concerned with the behaviour in tension of rat, bovine, or swine PDL (see, for instance, [Alatli et al. 1997; Pini et al. 2004; Dorow et al. 2003; Genna et al. 2008]). Some work exists concerning experiments on the viscous tensile/compressive behaviour of the PDL: most of it done on whole teeth, thereby making it difficult to isolate the purely mechanical contribution of the PDL [Qian et al. 2009; Papadopoulou et al. 2014], some on small samples with a relatively simple geometry [Sanctuary et al. 2005]. The dynamic viscoelastic shear behaviour of PDL has been studied experimentally in [Tanaka et al. 2007]. A review of the experimental work on PDL published until 2011 can be found in [Fill et al. 2011]. Nevertheless, a tremendous uncertainty still exists about even the simplest tensile behaviour of the PDL at constant, small loading velocity (appropriate, for instance, for orthodontic loading analyses), mainly due to the difficulty in defining reliable testing standards.

It is felt that more experimental work, possibly more systematic, should be performed, in order to obtain data useful both to dentists and to engineers. In this paper, the attention is mostly devoted to

mechanical aspects, and, in its first part, the results of some experiments will be presented, possibly useful to validate mechanical models. The results of these tests might also be useful in other related fields, such as the forced orthodontic extrusion of fractured roots, or other fractured root extraction processes.

A method for the experimental study of the PDL properties that might furnish information about its tensile stiffness and strength, but which might also provide some insight into a common activity in the dental field, could derive from the analysis of the force–displacement relationship obtained during the extraction of a tooth from its socket. Also this seemingly important aspect of dental mechanics has hardly been explored. Some results, in terms of forces only, are reported in [Chiba et al. 1980; Komatsu et al. 1990; Lehtinen and Ojala 1980; Ahel et al. 2006]. Nothing seems to exist in terms of displacements corresponding to applied forces. Numerical simulations of this process have been reported in [Gei et al. 2002] and [Genna 2006], but only as a way of verifying the performance of analytical models for the mechanical behaviour of the PDL, with no experimental results to be compared with.

The first direct purpose of this work is to provide information concerning experimentally determined force–displacement curves in the extraction of swine teeth from their sockets.

The second is to report the results given by the coupling of two separate models, developed previously, applied to the simulation of the extraction of teeth from their sockets, by means of the finite element method (FEM). The first model, illustrated in [Genna 2006], describes the PDL as a thin interface with a fibrous microstructure. The second model, proposed in an accompanying paper [Genna 2014], concerns a stress–stretch equation for a single collagen fibre, to be inserted as a basic ingredient into the first model. In its original version [Genna 2006], the interface model for the PDL made use of a simple, phenomenological equation for the stress–stretch behaviour of a single collagen fibre in tension, based on physically meaningless constitutive parameters. The model proposed in [Genna 2014], on the contrary, describes the mechanical behaviour of a collagen fibre in tension on the basis of constitutive parameters that, for the most part, have a precise physical meaning.

Both these models, for the single collagen fibre and for the PDL seen as a fibrous tissue, once fully developed and validated, could be of use for the study of several other situations of interest in biomechanics in general. With specific reference to dentistry, the first applications that come to the mind are orthodontic loading, analysis of centre of rotation, analysis of mechanical fields produced by several types of loading, both physiological and exceptional. Accurate information about the stress and strain fields produced by loading upon healthy teeth is expected to be of use also for the design of innovative dental implants, or similar devices, which should reproduce the physiological conditions much more closely than what happens with the currently used designs.

Finally, this work provides indirect information about the mechanical strength in tension of swine PDL, and, in general, about the dependence of the PDL mechanical behaviour in tension on several parameters, both mechanical and geometrical, that govern the analysed system.

2. Materials and methods

The experimental activity concerns the extraction of single-rooted swine canine teeth. All the tests have been run at the Dental Clinic of the University of Brescia, Italy. The testing machine was the Instron MicroTester 5848, an electromechanical instrument designed for uniaxial tests in biomechanical applications at low values of applied forces [Instron Corporation 2001].

Figure 1. A typical sample of a swine canine and surrounding portion of jawbone.

Forty-seven samples have been tested, obtained from portions of jaws of 12–15 month old swine. The choice of swine teeth derives from three main reasons:

- the Italian law forbids the use of human teeth for experimental research;
- after monkeys, pigs have the best compatibility with the human genome, and they have eating habits reasonably close to humans';
- the availability of freshly slaughtered material in the zone of Brescia.

Canines have been chosen so as to have roots as straight and smooth as possible, in order to facilitate the experimental procedure.

All the tested jaws have been taken within one hour from the slaughter of the animal. The portions including the canines have been cut (see Figure 1), polished of the largest possible portion of external soft tissues, immersed in physiologic solution, and put in a refrigerator at $+4.3°$ C for 24 hours. It was impossible to immediately run the tests, owing to the necessity of waiting for the nowadays-mandatory legal controls on the slaughtered animals before any research activity.

The jaw portions were clamped directly into the lower grips of the Instron MicroTester. The connection of the teeth to the testing machine was obtained by drilling a small hole, of 1.2 mm of diameter, into the tooth crown, therefore at a safe distance from the PDL, threading a metallic wire for orthodontic applications into it, and connecting the wire to the Instron grips by means of a steel part specifically designed. Figure 2 shows the final setup of a typical test.

The adopted wire type is made of a titanium alloy, with a rectangular cross-section of size 0.5334×0.635 mm (0.021×0.025 in). Preliminary tension tests on the wire gave an average material Young modulus equal to $E_t \approx 78000$ MPa.

It was not feasible, in the experimental arrangement devised so far, to always have a perfectly constant setup for the connecting wire, whose length was of about 50 mm, with possible small variations from test to test.

The smallness of the external portion of the tooth crown, together with the presence of residual soft tissues around the jawbone, made it impossible to connect an instrument capable of measuring the relative displacement between tooth and bone. Therefore, the only displacement measure available was the current distance between the machine grips.

Before extraction, each tooth was subjected to syndesmotomy, to a depth of 2 mm, using a Hu–Friedy syndesmotome. Without this preliminary operation, it was impossible to obtain a clean extraction, as either the wire, the tooth crown, or the jawbone broke prematurely.

The tests have been conducted prescribing the displacement of the upper grip in the machine, keeping the lower one fully fixed, at a rate of 2 mm/min. Forces have been measured with a uniaxial load cell with range of ± 2 kN.

3. Numerical models

The extraction process performed experimentally has been simulated by means of nonlinear FEM analyses. Several geometries of a tooth plus a surrounding portion of the jawbone have been considered, some of which describe swine canine teeth and others human incisors or two-rooted molars.

Figure 2. The testing setup.

3.1. *Numerical techniques.* All the numerical analyses have been run adopting the FEM as implemented in the partially open commercial code ABAQUS [Hibbitt et al. 2013].

After an initial geometrically nonlinear step, in which the initial slack of the titanium alloy wire is recovered, a second step applies traction to the tooth in a regime of small displacements, confining the geometrical nonlinearity to the formulation of the interface element for the PDL.

An interface finite element has been developed and coded into a Fortran 90 user subroutine UMAT to describe the nonlinear behaviour of the PDL, as proposed in [Genna 2006]. Each element is defined by six nodes, three of which are shared with a tetrahedral element describing the jawbone, and the other three with the adjacent tetrahedral element describing the tooth root. The nodal displacements are defined in a local reference system $n - t_1 - t_2$, where n is orthogonal to the bone surface, directed from bone to tooth root; t_1 is orthogonal to n and lies in a plane defined by n and the main axis of the tooth root; t_2 forms a right-handed reference system with the first two axes. The initial thickness of the PDL layer is denoted by w_0. Figure 3 shows both a sketch of a generic interface element and the microstructural arrangement underlying the assumed mechanical behaviour.

Figure 3. Sketch of the geometrical arrangement of the interface finite element for the description of the periodontal ligament. Left: nodes, intrinsic reference system, Gauss points. Right: diagram of the two wavy cables that define, at each Gauss point, the mechanical behaviour of the tissue.

At each of the three Gauss points of each interface element, the mechanical behaviour is governed by the existence of two cables. Both are inclined, in the undeformed configuration, by an angle β_0 with respect to the n axis, in the $n - t_1$ plane, and by an angle $\pm\theta_0$ with respect to the t_2 axis, in the $n - t_2$ plane. In this way, at each Gauss point the two cables are arranged into an X-shaped configuration in a transverse plane; this provides a torsional stiffness even for small displacements, since, upon the application of a torque around the main axis of the tooth, one of the two cables starts elongating immediately (see [Genna 2006]).

Each cable, in this model, represents a large random number of collagen fibres, having a wavy geometry at rest; the uncoiled, unstretched length of a single collagen fibre is denoted by L_b, which will be assumed to be a random variable. Each fibre starts furnishing an axial stiffness only when it is fully uncoiled; bending stiffness contributions of the fibres are neglected. The definition of the PDL compressive behaviour is obtained by a phenomenological equation devoid of physical meaning, and of no interest here.

Denote by l_0 the end-to-end distance between the extremities of each coiled fibre in the unstretched configuration, i.e.,

$$l_0 = w_0\sqrt{1 + \tan^2 \beta_0 + 1/\tan^2 \theta_0}. \tag{1}$$

Then the nondimensional variable x_c is introduced, defined as

$$x_c = \frac{L_b}{l_0}, \quad x_c \geq 1, \tag{2}$$

and assumed to be a random variable, whose probability density function $f_{x_c}(x_c)$ is here assumed to be of the gamma type, with known expected value and variance.

In order to obtain an expression for the expected value of the total macroscopic stress in each Gauss point of each interface element, for a given vector $\boldsymbol{\delta}$ of displacement jumps defined in the local reference system, the forces F_1 and F_2 existing in the two cables are computed through a statistical integration

over the admissible values taken by the random variable x_c of (2); i.e., denoting by $l_i(\boldsymbol{\delta})$, $i = 1, 2$, the current, stretched length of each cable, for $l_i(\boldsymbol{\delta}) > L_b$, we have

$$F_i(\boldsymbol{\delta}) = A_i \int_1^{l_i/l_0} \sigma_i(x_c, \boldsymbol{\delta}) f_{x_c}(x_c) \, dx_c, \quad i = 1, 2, \tag{3}$$

where $\sigma_i(x_c, \boldsymbol{\delta})$ indicates the local stress in a single collagen fibre for a given value of the displacement vector $\boldsymbol{\delta}$, and A_i indicates the cross-section area covered by all the fibres.

From (3), simple analytic developments lead to explicit expressions for the normal and shear stresses at each Gauss point of the interface element; in these expressions the areas A_i are accounted for by the volume fraction f_c of the stress-carrying portion of fibres, assumed to be known.

Equation (3) requires an expression for the local stress $\sigma_i(\boldsymbol{\delta})$ in a collagen fibre. In [Genna 2006] such an expression was provided by a simple nonlinear equation, with no physical meaning. Here, the microstructurally-based relationship proposed in the accompanying paper [Genna 2014] is adopted instead. Such a relationship requires, essentially, the calculation of a statistical integral of the type (3) also for obtaining the value of the local stress $\sigma_i(x_c, \boldsymbol{\delta})$.

This same stress–stretch expression automatically accounts for the tensile failure of the PDL because, after following a nonlinear increase of stress with elongation, it describes a stress peak and then a stress decrease due to the progressive failure of the shortest subfibrils, and finally reaches an irreversible zero stress value. From then on, the Gauss point gives no more mechanical contribution in tension.

According to these models, the mechanical behaviour of the PDL is nonlinear elastic–brittle, and time-dependency is neglected. This is a necessity, since both the adopted models — for the single collagen fibre, and for the PDL — are a first tentative description of the behaviour of these components, based on their microstructure: study is under way to include, among the basic mechanisms, also viscosity. On the other hand, and because of the short times involved by the tests, the specific problem herein analysed can be considered as inviscid as long as the material properties are obtained from tests performed at about the same loading velocity.

The reader is referred to [Genna 2006] for further details concerning the interface element formulation and implementation, and to [Genna 2014] for further details concerning the microstructurally-based stress–stretch equation for σ_i of (3).

3.2. *Geometries.* Figure 4 illustrates the four geometries considered in the numerical analyses. The first one, labelled (a), refers to one of the swine teeth extractions. The sample geometry has been acquired by means of a Sinergia Scan scanner, by Nobil–Metal Spa, which provides a surface point cloud with a resolution of $5 \, \mu\text{m}$. The point cloud has been transformed into a surface mesh, smoothed, and finally converted into a solid geometry by means of the code JRC 3D Reconstructor [Gexcel Src 2008].

The model includes the tested portion of the jaw, subdivided into cortical and spongious bones, the extracted canine tooth, and the titanium alloy wire adopted to connect the tooth to the testing machine. The jawbone is considered fully fixed to the reference system at a central portion that corresponds roughly to the size of the grips, and the top node of the wire is subjected to a prescribed displacement in the direction of the wire axis.

The remaining images in Figure 4 refer to human teeth. Image (b) refers to a two-rooted molar, whose geometry is taken from previous work [Corradi and Genna 2003]; image (c) to an incisor, also taken
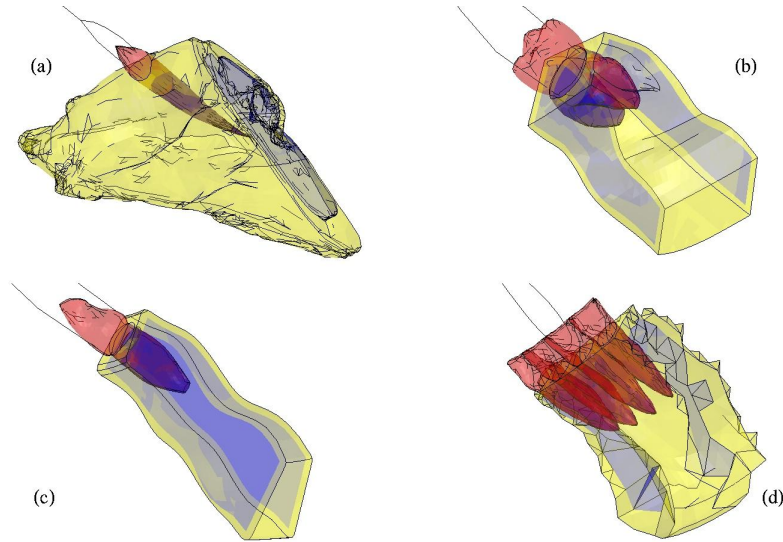
Figure 4. Geometries considered in the numerical analyses. (a) Swine canine, taken from a real sample; (b) human molar (schematic), taken from [Corradi and Genna 2003]; (c) human incisor (schematic), taken from [Corradi and Genna 2003]; (d) human incisor (schematic), from [Genna 2006]. The cortical bone is shown in yellow, the spongious bone in blue.

Tooth type	Height [mm]	Average diameter [mm]	PDL surface area [mm^2]
Swine canine (a)	29.32	4.26	292.04
Human molar (b)	15.04	6.50	240.76
Human incisor (c)	14.62	3.58	79.43
Human incisor (d)	21.19	4.22	160.18

Table 1. Geometrical data for the four tooth samples studied numerically.

from [Corradi and Genna 2003]; and image (d) corresponds to a different incisor, i.e., the same case, studied, by means of a simpler model, in [Genna 2006]. In all these analyses the boundary conditions are the same as described for the swine sample.

Table 1 reports the essential geometrical information about the four teeth studied numerically, i.e., sizes and areas of the root surfaces connected to the jawbone by the PDL.

3.3. *Materials.* In all the analyses, the bone, both cortical and spongious, and the dentine have always been described as linear elastic; the relevant material parameters are the same as those already adopted in [Genna 2006]. Also, the titanium alloy of the wire has been treated as linear elastic. The only nonlinear material, in all the numerical analyses, is the PDL layer, for which the following material parameters are required:

- the thickness w_0 of the PDL layer;
- the angles β_0 and θ_0 as defined above;

Material	Young's modulus [MPa]	Poisson's coefficient
Titanium alloy	78000	0.31
Dentine	20000	0.25
Cortical bone	13700	0.3
Spongious bone	1370	0.3

Table 2. Elastic properties of the jawbone and titanium alloy wire in the numerical models.

- the volume fraction f_c of stress-carrying collagen fibres inside the PDL;
- the expected value $E(x_c)$ and variance $\text{Var}(x_c)$ of the PDL collagen fibres waviness, described by the variable x_c introduced in Section 3.1;
- the data for the stress–stretch constitutive law of a single collagen fibre, that here correspond to the 19 parameters required by the model described in [Genna 2014]. The symbols and the relevant meanings are summarised here for convenience:
  - $N = 4$ is the number of internal levels defining the fibre microstructure;
  - K_s, K_m are the stiffnesses of a single tropocollagen molecule, described as a trilinear elastic–brittle rod;
  - X_{ks}, $X_{km} \geq 1$ are nondimensional coefficients that account for the effect of cross-linking on the fibre stiffness;
  - $X_f \geq 0$ is a nondimensional coefficient that describes the effect of cross-linking on the collagen brittle failure;
  - s is a molecular displacement related to the end of the second molecular stiffness range;
  - u_f^* is a molecular displacement related to the molecule failure;
  - Φ_m is the tropocollagen molecule diameter;
  - L_m is the contour length of a single tropocollagen molecule;
  - $f_0 f_1 f_2 f_3$ is the product of the volume fractions of the stress–carrying portion of internal sub-fibrils at the various internal levels of the collagen fibre microstructure (see [Genna 2014]);
  - $E(y_i)$, $\text{Var}(y_i)$ are the expected values and the variances, respectively, of the random variables $y(i)$, $i = 1, \ldots, N$, i.e., the nondimensional ratios that describe the waviness of the collagen subcomponents at the various internal levels;
- other parameters that define the compressive behaviour of the PDL, of no interest here.

Table 2 summarises the values of the elastic parameters for the two bone types, the dentine, and the titanium alloy wire.

Table 3 reports the numerical values of all the adopted material parameters for the description of the PDL. The thickness w_0 of the PDL layer has been varied, in some analyses, to verify its effect on the resulting force–displacement curves. Following the results presented in [Genna et al. 2008], for swine PDL the value $w_0 = 0.50$ mm has been adopted as a reference one, although in several cases higher values — up to about 1 mm — have been measured.

The values adopted for the angle β_0 depend on the position, along the tooth root axis, of each considered Gauss point, according to the geometrical information that can be found in the literature for human teeth [Berkovitz et al. 1995], and are the same as those adopted in [Genna 2006]. In the absence of better

Material parameter	Adopted value	Material parameter	Adopted value	Material parameter	Adopted value
w_0	swine: 0.50 mm	$E(y_2)$	0.9952	Φ_m	1.5 nm
	human: 0.25 to 1.0 mm	$E(y_3)$	0.99779	L_m	301.7 nm
β_0	$-25°$ to $30°$	$E(y_4)$	0.9979	s	50 nm
θ_0	$76.8°$ to $90°$	$\text{Var}(y_2)$	$4.9 \cdot 10^{-5}$	u_f^*	167 nm
f_c	0.05	$\text{Var}(y_3)$	$6.561 \cdot 10^{-5}$	L_b	random variable
$E(x_c)$	1.093	$\text{Var}(y_4)$	$3.387 \cdot 10^{-5}$	X_{ks}	1
$\text{Var}(x_c)$	0.00397	$f_0 f_1 f_2 f_3$	0.05	X_{km}	1
$E(y_1)$	0.995	K_s	10 pN/nm	X_f	0
$\text{Var}(y_1)$	$2.5 \cdot 10^{-5}$	K_m	30 pN/nm		

Table 3. Material parameters required by the periodontal ligament model.

information, the same values have been adopted also for the swine canine.

In Table 3, the parameter L_b, which denotes the uncoiled, unstretched length of a single collagen fibre at rest, is marked as a random variable, since its value depends on the statistics of the waviness of the fibres, i.e., on the current values of x_c of (2) during the integration process.

4. Results

4.1. *Experimental results.* Of the forty-seven tests, only sixteen concluded with the successful extraction of the tooth from its socket. All the other ones ended prematurely either because of wire failure or because of the failure of the tooth crown, due to the propagation of a crack initiated by the drilled hole.

Of these successful sixteen tests, all producing scattered results because of the inevitable differences among specimens, only seven cases have been considered as fully significant. The other ones produced even more dispersed results, either because the teeth were somehow defective or too small, so as to produce extraction forces far too small, or because they were affected by an excessive interference with the tissues — including soft ones — surrounding the extracted tooth, as indicated by the extremely large values of the displacement corresponding to the peak forces.

Figure 5 shows the obtained force–displacement curves for the best seven cases. The peak forces found experimentally are in the range 100 to 450 N, and the corresponding displacements are in the range 1 to 4.6 mm.

Beside the absolute values of stiffness (from about 20 to about 150 N/mm, depending on the samples, in the initial region), peak force, and peak displacement, another significant feature of all the curves of Figure 5 is the presence of several local peaks of force, both before and after the absolute maximum. Some of the peaks after the absolute maximum force may have little importance, since they are probably due to the existence of gingival or bone tissue that stays connected to the tooth even after its detachment from the socket, as shown in Figure 6. This residual connection might also be responsible for some extremely large displacement values found before the full drop of the force value to zero.

The force peaks before the absolute maximum, and some after it, are due to the variable inclination of the PDL collagen fibres along the tooth root, as will be shown in Section 5.
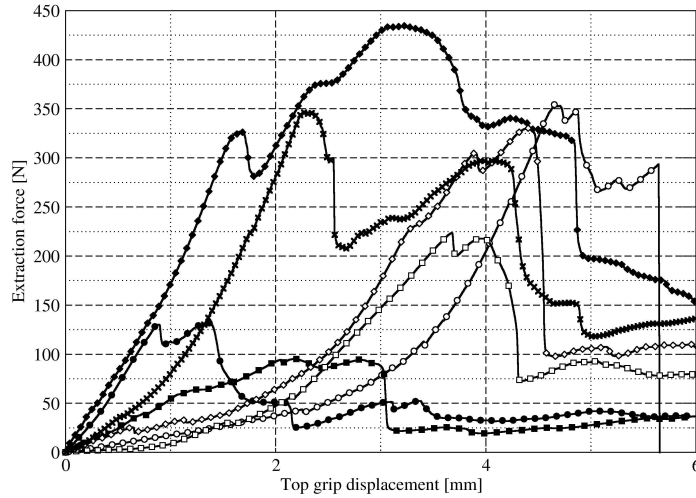
Figure 5. Experimental results from the tests on swine canines. In ordinate: force measured by the testing machine; in abscissa: grip opening displacement.
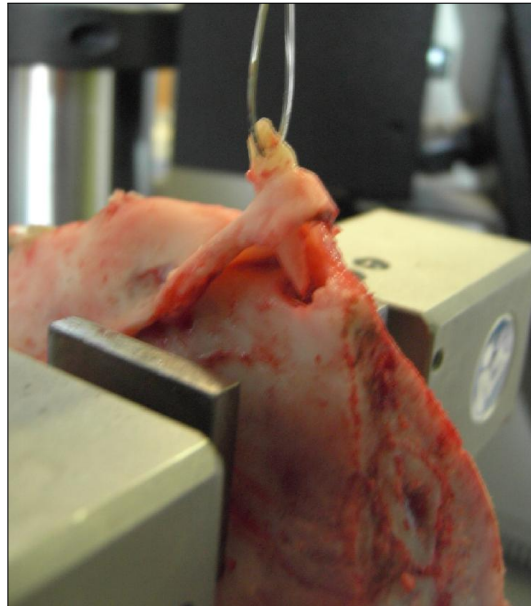
Figure 6. Tissues remaining connected to the swine canine after its extraction from the socket.

4.2. *Numerical results.* Figure 7 illustrates the first numerical result, which refers to the simulation of the extraction of a swine canine, performed on the geometry of Figure 4(a). In this analysis, the PDL thickness was set equal to $w_0 = 0.5\,\text{mm}$. Figure 8 compares the numerical results obtained for the simulation of the extraction of human teeth on the geometries of Figure 4(b), (c), and (d); in all these cases the PDL thickness was set equal to $w_0 = 0.25\,\text{mm}$.
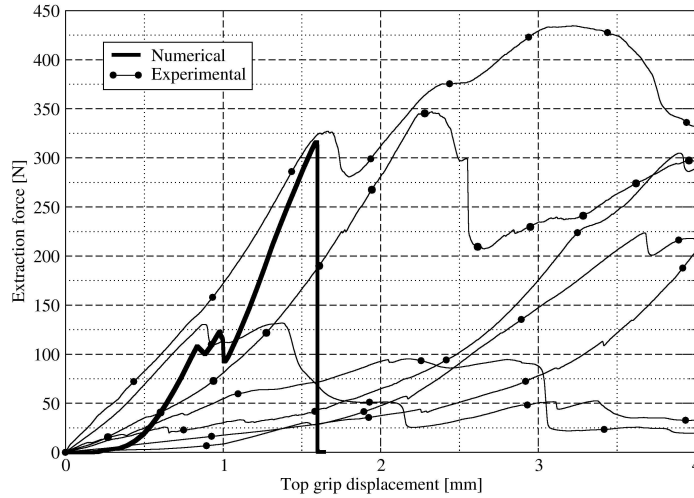
Figure 7. Swine canine extraction: comparison between experimental and numerical results. The thick solid curve is obtained numerically, from the approach presented in this work. All the remaining curves, with black circles, are experimental results already shown in Figure 5.
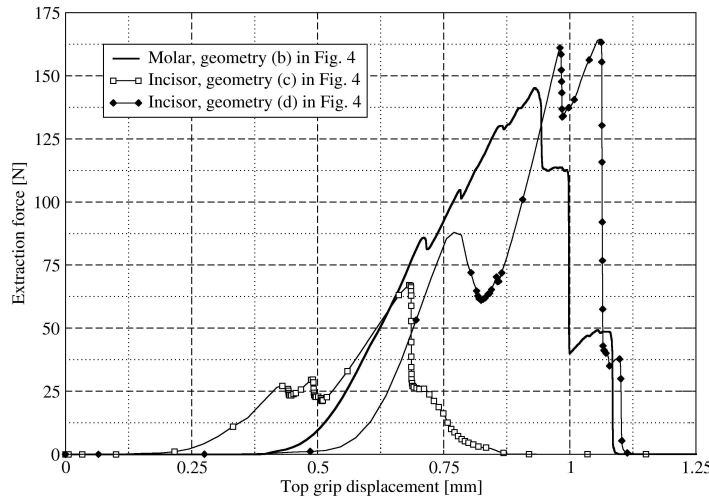
Figure 8. Numerical results: comparison among different geometries for human teeth. The solid curve refers to the molar of Figure 4(b); the curve with white squares refers to the geometry of Figure 4(c); and the curve with black diamonds refers to the geometry of Figure 4(d).

Figures 9 and 10 show, respectively, the influence of the PDL thickness on the computed force–displacement extraction curve, and the influence of the wire stiffness on the same curve. Figure 9 shows results obtained from the same geometry (that of Figure 4(c)), by varying the adopted value for the PDL thickness w_0. Figure 10 presents two plots, both referring to the same simulation, i.e., the case of the
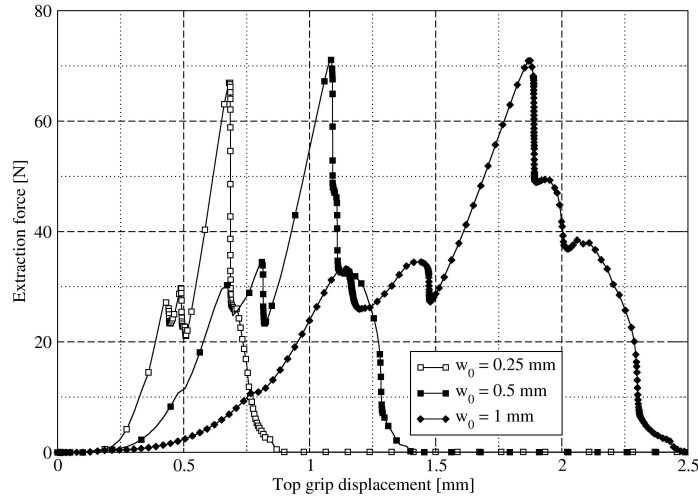
Figure 9. Numerical results: effect of the PDL thickness w_0 on the computed force–displacement curves. The geometry is that of Figure 4(c) (human incisor).
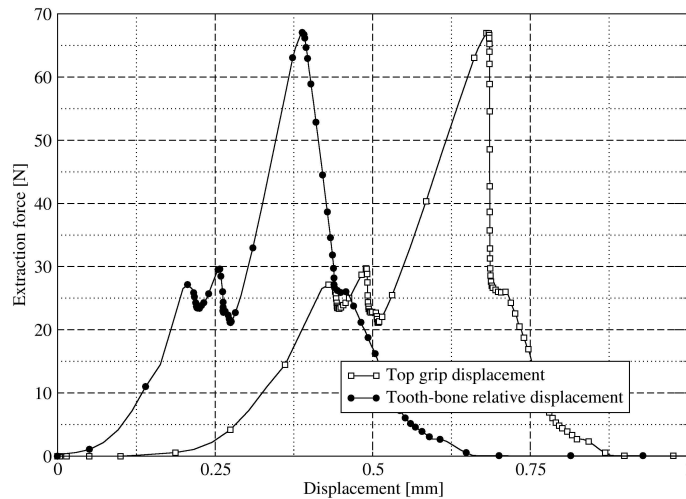
Figure 10. Numerical results: effect of the stiffness of the connecting wire on the computed force–displacement curves. The geometry is that of Figure 4(c) (human incisor).

human incisor of Figure 4(c), with $w_0 = 0.25$ mm: the first curve is the same as in Figure 8, the second curve plots the same force as a function of the relative displacement between the root crown and the top surface of the cortical bone around the tooth itself.

Finally, Figure 11 illustrates the effect produced by the variation of the PDL fibre inclination, along the tooth root, on the force–displacement curve. The plots refer to the case of the human incisor of Figure 4(c), with $w_0 = 0.25$ mm; the first one coincides with that of Figure 8, the second one is obtained by setting $\beta_0 = 0$ and $\theta_0 = 90°$ in the PDL constitutive parameters, i.e., fixed fibre direction, orthogonal to the root external surface, and with no X-shaped transversal arrangement.
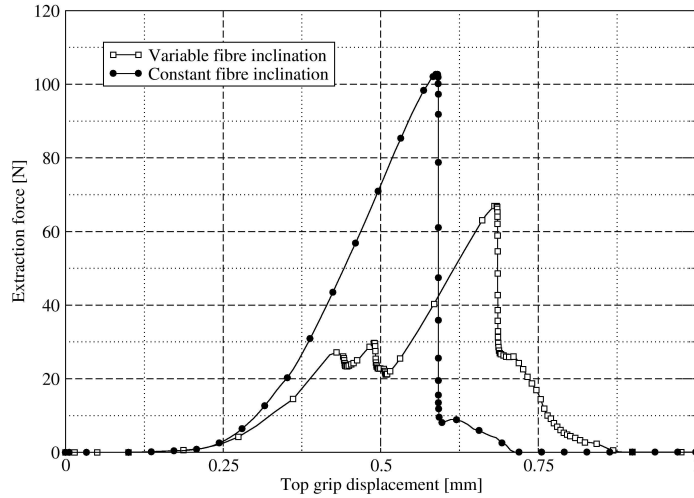
Figure 11. Numerical results: effect of the inclinations β_0 and θ_0, shown in Figure 3, on the computed force–displacement curves. The geometry is that of Figure 4(c) (human incisor). The curve with white squares is the same as the one in Figure 8, with "realistic" values for both β_0 and θ_0. The curve with black dots is obtained by setting $\beta_0 = 0°$ and $\theta_0 = 90°$ at all the interface elements.
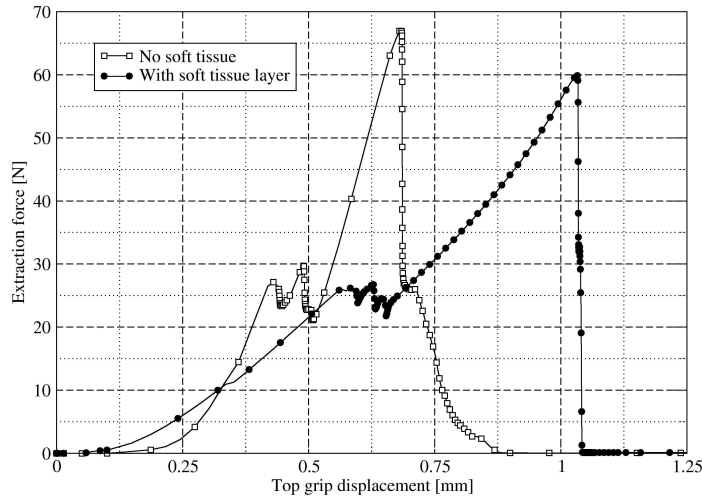
Figure 12. Numerical results: effect of the stiffness of a thin layer of soft tissue around the jawbone on the computed force–displacement curves. The geometry is that of Figure 4(c) (human incisor).

The size of the discretised numerical problem has always been in the range of 30 000 to 50 000 degrees of freedom, depending on the considered model. The CPU times, on a Hewlett–Packard workstation xw9300, with 2 AMD Opteron 64-bit dual-core processors, but no parallel processing exploited, have

been of the order of 3 hours for all the cases. This demonstrates the practical usability of the constitutive model adopted for the single collagen fibre proposed in [Genna 2014].

5. Discussion

The experimental force–displacement curves shown in this paper are obtained by means of a technique that differs from the one adopted in real dental practice: the tooth has simply been pulled out of the socket, whereas the standard procedure involves applying a luxation, with leverage and torsion. It is currently impossible to understand the extent of the possible differences in the force and displacement values due to this discrepancy.

Moreover, the choice of extracting only single-rooted canines has somehow limited the range of results that could possibly be obtained. On the other hand, it has to be considered that, quite often, the extraction of two- or three-rooted teeth, or of teeth having roots with a complex/defective geometry, results in breaking either the socket bone or the root itself: this would have been a useless complication in our case.

Both a significant dispersion even in the best experimental results, and a lack of an established standard for the experimental technique are apparent. The last difficulty could not be avoided, in view of the complete novelty of the performed tests; it would be desirable to establish a standard procedure even for tooth extraction laboratory tests, but the extreme variability of all the factors involved makes this a quite difficult task, and anyway outside the scope of this work.

As for the scatter in the measured force–displacement curves, it should be noted that each curve refers to a completely different sample, taken from a different animal, each with its own physical and geometrical properties. The dispersion of the results is similar to that obtained in the past from experiments, in a much more controlled regime, performed on small PDL samples, such as those of [Genna et al. 2008] and [Pini et al. 2004]. The situation, in the case of large mandible blocks and full teeth, is understandably more dispersed.

The experimental setup seems to influence mainly the displacement values, but to provide reliable values for the extraction forces. This is also confirmed by considering the average stress values corresponding to the peak extraction force, obtained by dividing the force by the root area. Adopting an average value for the root surface area equal to $143 \, \text{mm}^2$ as given by the tests, and considering the observed range of peak force values, i.e., 100 to 450 N, one obtains average values for the fracture stresses of the PDL in the range 0.7 to 3.2 MPa, in good agreement with the experimental results on swine PDL samples reported in [Genna et al. 2008].

Both the observed and the computed peaks of force fall within the range of values that can be found in the literature; nevertheless, the results presented here seem to be the first that have been obtained directly from an extraction test performed by means of a standard testing machine capable of measuring both forces and displacements. The few results previously available are all obtained in somewhat indirect ways, such as, for instance, those presented in [Ahel et al. 2006], where a forceps was instrumented in such a way as to obtain "pressure and rotation measurements".

Figure 9 shows that larger values of the PDL thickness produce larger displacements at about the same force values. This might help in explaining some of the larger values of displacements recorded in the laboratory tests: swine PDL can be much thicker than human one, according to the available information, and its thickness gives a clear contribution to the overall stiffness of the tooth-PDL-bone system.

The comparison of the curves shown in Figure 11 illustrates an important effect of the PDL collagen fibre inclination, and especially so for single-rooted teeth. In the real situation the fibres are arranged so as to withstand all the possible types of loading, always offering stiffness due to their being stretched. The fibres that first offer stiffness, upon an axial pulling displacement of the tooth, are those more aligned with the loading direction, while all the others will undergo either a rigid rotation, or milder stretching. Increasing the tooth axial displacement will eventually lead to the failure of the most stretched fibres, thus causing a local drop in the global extraction force. Thereafter, other groups of fibres will start becoming aligned with the loading direction, and offering stiffness, thus causing a new force increase. This effect is shown by the numerical results, which, for the case of a fixed fibre inclination along the root, do not show any local force maximum.

In the case of molars, the variable inclination of the collagen fibres is less important, because the root surface is not convex. In fact, even considering $\beta_0 = 0°$ and $\theta_0 = \pm 90°$, in a numerical simulation of the extraction of molars, one would obtain at least a local peak of force before the absolute maximum, corresponding to the failure of the interradicular fibres located between the roots, in the internal concave zone under the tooth crown. These fibres, with $\beta_0 = 0°$, are practically aligned with the root axis in the undeformed configuration, and would be the first to stretch and break.

The numerical simulations are based on mathematical models for both the PDL as a tissue, and a single collagen fibre as its basic constituent, developed from the same basic idea, i.e., to describe in the simplest possible way both the tissue and the fibre microstructure. Of course, for both the PDL and the collagen fibres many other mathematical models exist in the literature, although, to the best of our knowledge, none of them has a micromechanical basis. There is no space here (and this is not the proper place, also) to review the existing literature; the interested reader is referred to the list of references in [Genna 2014] for collagen, and to [Fill et al. 2012; Romanyk et al. 2013], and the list of references in [Genna 2006], for the PDL.

In all the force–displacement plots illustrated in the previous section, the influence of the wire stiffness and initial slack is quite important, as explicitly shown also by Figure 10. Beside this aspect, one must also consider that, in the experiments, the lower grips of the testing machine were connected to a block of bone which contained residual portions of soft tissues, whose influence on the recorded displacements might be nonnegligible. In order to quantify this aspect, a second FEM analysis for the case of the human incisor of Figure 4(c) was run, in which the cortical bone was surrounded by a thin layer (0.5 mm thick) of soft tissue, whose mechanical behaviour was simulated by means of a hyperelastic model of the Ogden type, with a quadratic potential function.

Figure 12 shows the comparison between the force–displacement curves obtained with and without the soft tissue around the cortical bone: it is apparent that even a very thin layer of very compliant material can increase the displacement at the peak force by about 60%, with a slight decrease of peak force value.

It is also interesting to observe that the numerical simulations, even when they take into account several factors that might increase the overall compliance, always tend to underestimate the displacement corresponding to the maximum force, with respect to the experimental results. It must be recalled that the material parameter choice in the description of the PDL collagen corresponds to a very large ductility, with uniaxial Green–Lagrange strain at peak stress of the order of 1.2 for the PDL layer, as shown in Figure 8 of [Genna 2014], and uniaxial Biot strain at peak stress of the order of 0.55 for a single collagen fibre, as was also necessary when adopting the different model presented in [Genna 2006]. In

the numerical simulations presented here, cross-linking in the PDL collagen has always assumed to be absent, which corresponds to the highest possible values of strains at failure in the collagen fibres [Pins et al. 1997] in the adopted model; yet, the global behaviour obtained from the FEM simulations, as said, always shows an underestimated ductility with respect to the experimental one. Even the case expected to produce the largest displacement at the force peak, i.e., one in which both the wire and the thin layer of soft tissue are present, with the largest among the adopted values of the PDL thickness ($w_0 = 1$ mm), yields a displacement value of 2.3 mm at the force peak, smaller than most of the experimental values.

The large displacement values obtained experimentally seem therefore to confirm the corresponding high strain values that can be reached by the PDL collagen fibres before failure.

6. Conclusions

For the first time, to the best of the authors' knowledge, force–displacement curves have been obtained experimentally from the process of extraction of swine teeth from their sockets. The experimental setup adopted allows the use of a standard testing machine, thus providing direct values of both forces and displacements. Nevertheless, at the current stage of development it is not yet fully standardised so as to provide results substantially independent of the testing apparatus itself. Work is in progress in two main respects: the inclusion of a "rigid" connection between tooth and machine grip, and the measurement of the relative displacement between tooth and bone, possibly through optical devices.

The results herein presented are expected to be useful to developers of mathematical models for the PDL, since they provide at least some indirect information (for instance, about the fibre inclination) on the mechanical and geometrical properties of the PDL.

The numerical analysis of the same problem has shown the ability to obtain meaningful results, and has also proven the practical applicability of the constitutive model for a single collagen fibre proposed in an accompanying paper [Genna 2014].

Further work, in this respect, should tackle the problem of the PDL behaviour under small and cyclic loading, which will require taking into account irreversible and time-dependent effects. With respect to these last, we point out that, for simplicity in this initial stage, the experimental program carried out so far did not investigate the effect of the loading, i.e., displacement, rate, which was always kept constant, at 2 mm/min. Although slower loads could be successfully applied with the adopted setup, faster ones could not, since they would produce premature ending of the experiment due to fracture either of the wire or of the tooth crown.

Acknowledgements

References

[Ahel et al. 2006] V. Ahel, I. Brekalo, J. Ahel, and G. Brumini, "Measurements of tooth extraction forces in upper incisors", *Coll. Anthropol.* **30**:1 (2006), 31–35.

[Alatli et al. 1997] I. Alatli, J. Li, and L. Hammarström, "Ultimate tensile strength of PDL of molars in rats after 1-hydroxy-ethylidene-1, 1-bisphosphonate injections", *J. Dent.* **25**:3-4 (1997), 313–319.

[Berkovitz et al. 1995] B. K. B. Berkovitz, B. J. Moxham, and H. N. Newman, *The periodontal ligament in health and disease*, 2nd ed., Mosby-Wolfe, London, 1995.

[Chiba et al. 1980] M. Chiba, S. Ohshima, and K. Takizawa, "Measurement of force required to extract the mandibular incisor of rats of various ages", *Arch. Oral Biol.* **25**:10 (1980), 683–687.

[Corradi and Genna 2003] L. Corradi and F. Genna, "Finite element analysis of the jaw-teeth/dental implant system: A note about geometrical and material modeling", *Comput. Model. Eng. Sci.* **4**:3 (2003), 381–396.

[Dorow et al. 2003] C. Dorow, N. Krstin, and F. Sander, "Determination of the mechanical properties of the periodontal ligament in a uniaxial tensional experiment", *J. Orofac. Orthop.* **64**:2 (2003), 100–107.

[Fill et al. 2011] T. S. Fill, J. P. Carey, R. W. Toogood, and P. W. Major, "Experimentally determined mechanical properties of, and models for, the periodontal ligament: Critical review of the current literature", *J. Dent. Biomech.* **2**:1 (2011), Article ID 312980.

[Fill et al. 2012] T. S. Fill, R. W. Toogood, P. W. Major, and J. P. Carey, "Analytically determined mechanical properties of, and models for the periodontal ligament: Critical review of literature", *J. Biomech.* **45**:1 (2012), 9–16.

[Gei et al. 2002] M. Gei, F. Genna, and D. Bigoni, "An interface model for the periodontal ligament", *J. Biomech. Eng. ASME* **124**:5 (2002), 538–546.

[Genna 2006] F. Genna, "A micromechanically-based, three-dimensional interface finite element for the modeling of the periodontal ligament", *Comput. Methods Biomech. Biomed. Engin.* **9**:4 (2006), 243–256.

[Genna 2014] F. Genna, "A nonlinear stress-stretch relationship for a single collagen fibre in tension", *J. Mech. Mater. Struct.* **9**:5 (2014).

[Genna et al. 2008] F. Genna, L. Annovazzi, C. Bonesi, P. Fogazzi, and C. Paganelli, "On the experimental determination of some mechanical properties of porcine periodontal ligament", *Meccanica* **43**:1 (2008), 55–73.

[Gexcel Src 2008] *JRC 3D Reconstructor*, Gexcel Src, Brescia, Italy, 2008, http://www.gexcel.it/en/lidar-software-solutions/reconstructor-full.

[Hibbitt et al. 2013] H. D. Hibbitt, B. Karlsson, and P. Sorensen, *Abaqus user's manuals, Release 6.12*, Dassault Systèmes, Simulia Corp., Providence, RI, 2013.

[Instron Corporation 2001] *Instron model 5848 MicroTester: Reference manual—equipment*, Instron Corporation, Norwood, MA, 2001, http://www.instron.us/wa/library/StreamFile.aspx?doc=808.

[Komatsu et al. 1990] K. Komatsu, S. Ohshima, and M. Chiba, "Measurement of force required to extract the mandibular first molar from its socket in the dissected jaw of growing young rats", *Gerodontology* **9**:1 (1990), 3–7.

[Lehtinen and Ojala 1980] R. Lehtinen and T. Ojala, "Rocking and twisting moments in extraction of teeth in the upper jaw", *Int. J. Oral Surg.* **9**:5 (1980), 377–382.

[Papadopoulou et al. 2014] K. Papadopoulou, L. Keilig, T. Eliades, R. Krause, A. Jäger, and C. Bourauel, "The time-dependent biomechanical behaviour of the periodontal ligament—an *in vitro* experimental study in minipig mandibular two-rooted premolars", *Eur. J. Orthod.* **36**:1 (2014), 9–15.

[Pini et al. 2004] M. Pini, P. Zysset, J. Botsis, and R. Contro, "Tensile and compressive behaviour of the bovine periodontal ligament", *J. Biomech.* **37**:1 (2004), 111–119.

[Pins et al. 1997] G. Pins, E. Huang, D. Christiansen, and F. Silver, "Effects of static axial strain on the tensile properties and failure mechanisms of self-assembled collagen fibers", *J. Appl. Polym. Sci.* **63**:11 (1997), 1429–1440.

[Qian et al. 2009] L. Qian, M. Todo, Y. Morita, Y. Matsushita, and K. Koyano, "Deformation analysis of the periodontium considering the viscoelasticity of the periodontal ligament", *Dent. Mater.* **25**:10 (2009), 1285–1292.

[Romanyk et al. 2013] D. L. Romanyk, G. W. Melenka, and J. P. Carey, "Modeling stress–relaxation behavior of the periodontal ligament during the initial phase of orthodontic treatment", *J. Biomech. Eng. ASME* **135**:9 (2013), 1–8.

[Sanctuary et al. 2005] C. S. Sanctuary, H. W. A. Wiskott, J. Justiz, J. Botsis, and U. C. Belser, "In vitro time-dependent response of periodontal ligament to mechanical loading", *J. Appl. Physiol.* **99**:6 (2005), 2369–2378.

[Tanaka et al. 2007] E. Tanaka, T. Inubushi, K. Takahashi, M. Shirakura, R. Sano, D. A. Dalla-Bona, A. Nakajima, T. M. G. J. van Eijden, and K. Tanne, "Dynamic shear properties of the porcine molar periodontal ligament", *J. Biomech.* **40**:7 (2007), 1477–1483.

FRANCESCO GENNA: francesco.genna@unibs.it
Department of Civil Engineering, University of Brescia, Via Branze 43, I-25123 Brescia, Italy

CORRADO PAGANELLI: corrado.paganelli@unibs.it
Dental Clinic, University of Brescia, Piazzale Spedali Civili, 1, I-25123 Brescia, Italy

JOURNAL OF MECHANICS OF MATERIALS AND STRUCTURES

msp.org/jomms

Founded by Charles R. Steele and Marie-Louise Steele

Cover photo: Wikimedia Commons

Journal of Mechanics of Materials and Structures